ELSEVIER

Nuclear Instruments and Methods in Physics Research Section B: Beam Interactions with Materials and Atoms

Volume 540, July 2023, Pages 246-258

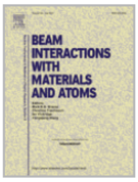

Thermoluminescence dosimetric and kinetic characterization of Pakistani fluorite after β irradiation

Mirza Wazir-ud-Din [a], Shakeel-ur-Rehman [a], Dirk Poelman [b], Johan De Grave [c], Dimitri Vandenberghe [c], Muhammad Basim Kakakhel [a], Sikander Hayat [a], Nasrin Karimi Moayed [c]

Show more

+ Add to Mendeley Share Cite

https://doi.org/10.1016/j.nimb.2023.04.031

Thermoluminescence dosimetric and kinetic characterization of Pakistani fluorite after β irradiation

Mirza Wazir-ud-Din [a], Shakeel-ur-Rehman [a], Dirk Poelman [b], Johan De Grave [c], Dimitri Vandenberghe [c], Muhammad Basim Kakakhel [a], Sikander Hayat [a], Nasrin Karimi Moayed [c]

[a] Department of Physics & Applied Mathematics, Pakistan Institute of Engineering and Applied Sciences (PIEAS), Islamabad 45650, Pakistan

[b] LumiLab, Department of Solid State Sciences, Ghent University, Krijgslaan 281 (S1), B-9000 Gent, Belgium

[c] Laboratory of Mineralogy and Petrology, Department of Geology, Ghent University, Krijgslaan 281 (S8), B-9000 Gent, Belgium

Abstract

The thermoluminescence (TL) characteristics of seven fluorite mineral samples from Pakistan have been investigated for the first time. The TL glow curve structure of different colors of fluorite were thoroughly studied for their potential use in dosimetric applications. Light green (LG) fluorite was found the most sensitive and promising one. Therefore, light green (LG) fluorite was further investigated in detail as TL dosimeter. First, the crystallinity, microstructural properties, and potential impurities present in the LG sample were identified using *x-ray powder diffraction (XRD), Scanning electron microscopy (SEM-EDX),* and *inductively coupled plasma (CP)* techniques respectively. The

β-irradiated powder sample showed that this fluorite has a complex glow curve structure with five prominent peaks at about 75, 100, 163, 251, and 358°C in the temperature range of 40 to 400°C. In the low β dose range of 80 mGy to 5120 mGy, the sample dose response was linear with a minimum detectable dose of 9.7 mGy. Taking the peak specific dose responses, the peak around 251°C (R^2 = 1) was found most suitable for dosimetric applications. A progressive decrease is observed in the response which reached to about 4% after 10 cycles of irradiation, readout and annealing with less than 1% coefficient of variation (COV). After one week, the TL signal faded by approximately 8%; however, after one month of storage, the signal returned to near-stable level. A newly designed deconvolution program was used for the analysis of the TL kinetics. The kinetic parameters like activation energy (E), frequency factor (s), the order of kinetics (b), and the trap lifetimes were investigated. The values found using additive dose (*AD*), T_m -T_{stop}, various heating rate (*VHR*) and computerized glow curve deconvolution (*CGCD*) methods were in close proximity. The study concludes that light green fluorite from Pakistan can be used as a potential candidate for thermoluminescence dosimetry (TLD) applications.

1 Introduction

Thermoluminescence (TL) is the thermally stimulated emission of light from an insulator or semiconductor following the previous absorption of energy from radiation. This phenomenon is observed in many natural and synthetic materials [1, 2]. Radiation monitoring and dosimetry using this phenomenon have been under study since the discovery of radiation effects [3-6].

The charge carriers (i.e., electrons and holes) responsible for TL, are trapped at the defect sites in these materials. These defects or traps may be present inherently like F-Centers (lattice vacancies occupied by one or more electrons) or can be produced deliberately by doping the material with some impurity atoms e.g. LiF: Mg, Ti [7, 8].

Several minerals have been reported as TL dosimetric material due to their unique TL properties which ultimately depend on the geological processes during formation times [7, 9-15]. Fluorite (natural CaF2) is only one of them having a Face-Centred Cubic (FCC) structure and is non-hygroscopic in nature. Sintered and Single-Crystal pellets of synthetic and doped CaF_2 (with one or more rare earth elements i.e. CaF2: Dy as TLD-200, CaF2: Tm as TLD-300 or transition elements i.e. CaF2: Mn as TLD-400) variants are probably known best and are commercially available from Harshaw Chemical Co[16] .

Schayes *et al*. have performed a comprehensive study of fluorite [17, 18] and subsequently, many authors investigated its other TL properties [19, 20]. They reported it a highly sensitive and cost-effective TL dosimetric material with linear response and emission in the maximum efficiency region of photomultiplier tubes (PMT) present in most TL readers. Some recent studies have extended the TL properties of fluorite. Balogun *et al*. suggested that the formation of large defect complexes in fluorite is responsible for peak response changes with storage time [21]. Ogundare *et al.* identified the kinetic parameters of the main dosimetric peaks of Nigerian fluorite [22]. Kitis *et al.* and Ogundare *et al.* discussed the effect of the heating rate on the TL glow curve shape and the integrated response of fluorite respectively [23, 24].

Studies on the spectral analysis of TL explain the emission mechanism from this natural phosphor. The occurrence of radiation induced defects is probably due to changes in the valence state from +3 to +2 of the rare earth elements (REEs) or the transformation of structural defects upon exposure to ionizing radiation [25, 26]. The type and percentage of the developed traps depend upon the host crystal's geological site, origin, and growth conditions. These conditions vary from one deposit to another, rendering the peak height and position in the glow curve [21, 22, 27]. Fluorite is one of the minerals in the earth's crust with a variety of hues/colors such as black, purple, green, violet, white, brown, yellow, etc. These colored fluorites contain one or more REE activators which are primarily responsible for the TL emission at different temperatures [28, 29].

Similar to other global deposits, the Indus Basin of Pakistan also contain a large quantity of fluorite of various colors [30]. The widespread availability, low cost of exploration and ease of production, and high grade of concentration of this TL material make it an attractive candidate for use in radiation dosimetry and monitoring, especially for developing countries like Pakistan. In this study, we first examined the glow curve structure and sensitivity of seven colored fluorites (white, pink, purple, black, blue, green, and light green). The light-green variant showed the highest luminescence sensitivity. We then characterized this material in terms of mineralogical and chemical composition, and TL dosimetric properties and kinetic parameters. This is the first time that fluorite samples from the Indus Basin in Pakistan have been studied for luminescence dosimetric purposes.

2 Materials and Methods

2.1 Sample Collection, Preparation and storage

The Indus Basin of Pakistan holds a variety of economically significant tectonic, metamorphic and sedimentary minerals (Figure 1). New fluorite deposits of approximately 50000 tons have been found in the Jurassic Loralai limestone of Gadebar, Daman Ghar, Tor Thana, Wategam, Mekhtar, Balao, and Mahiwal areas of Loralai District, Baluchistan. The fluorite of the Loralai area occurs as veins and disseminated grains along faults and fractures and can be used for acid preparation and as gemstones having CaF_2 content of up to 95%.[31].

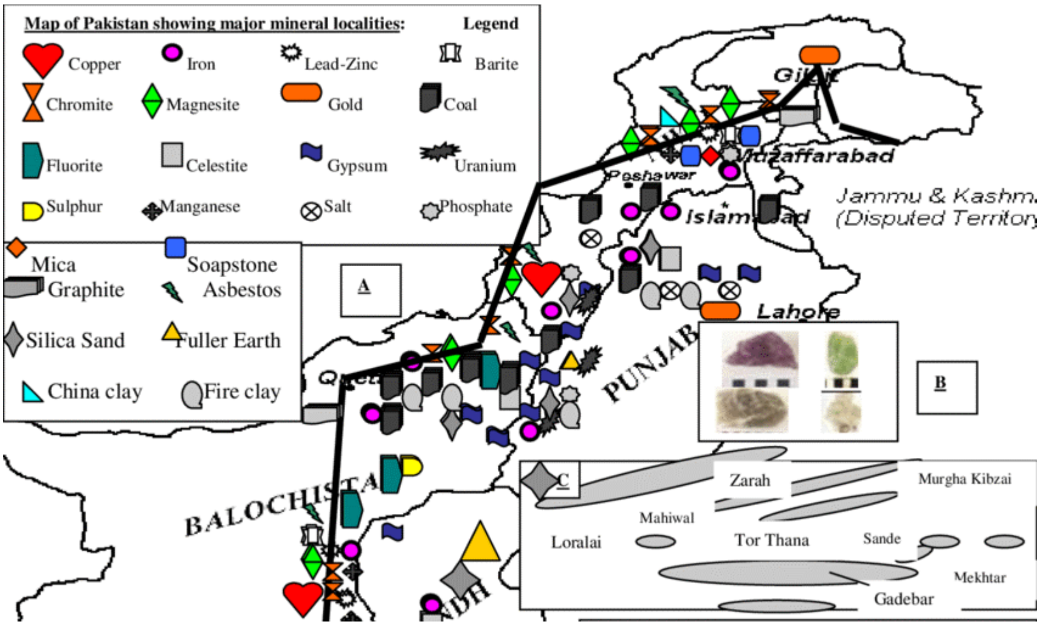

Figure 1: (A) Major minerals and their location in map of Pakistan, (B) different colors of fluorite samples and (C) specific regions of sample collection in Balochistan Province [31]

Samples of Fluorite with different colors (white, pink, purple, black, blue, green, and light green) from different mines of Loralai and adjacent districts of Baluchistan (Pakistan) were provided by the Pakistan Museum of Natural History, Islamabad. Optically selected pieces of fluorite crystal were washed thoroughly with fresh water and dried. A Retsch Mortar Grinder RM 200 using Agate Mortar-Pestle was used for reproducible analytical results. Grain sizes from 63-180 μm were separated for further studies. Sunta showed that fluorite is a light-sensitive material and its TL response varies with exposure time and intensity [29]. As a result, all samples were stored in a dark room, and all experiments were undertaken in the dark, to prevent any possible changes caused by light exposure.

2.2 Material characterization

Material characterization techniques play an important role in identifying the main signatures of the sample. The mineralogy and crystalline structural analysis of the bulk powder form of the fluorite sample was examined using a Bruker D5000 X-ray diffractometer equipped with a copper target (Kα, λ = 1.54186 Å). The measurements were taken in the 2θ angular range of 5-90°, with a step size of 0.02 degrees and scan step time of 0.4 seconds. X'Pert HighScore Plus analysis software along with the International Center for Diffraction Data (ICDD) 2003 PDF2 database was employed for the analysis of the XRD patterns. The crystallite size was calculate using Scherrer formula [32] as given below

$$Crystallite\ Size(\tau) = K\lambda/\beta cos\theta \tag{1}$$

where τ is the size of the particle, K is Scherer's constant (K=0.94), λ is the X-ray wavelength, θ is the angle of diffraction, and β is full width at half maximum (FWHM) of the diffraction peak. Chemical analysis of the major and minor elements was carried out by of iCAP 6500 (Thermo Fisher Scientific, UK) Inductively Coupled Plasma Optical Emission Spectrometry (ICP-OES). For morphological studies, a field emission scanning electron microscope (FE-SEM) with an Octane Elite EDAX detector is used to examine the elemental concentration and the powder surface morphology.

2.3 Pre-irradiation thermal treatment

It is well known that heat treatment or annealing is essential before any irradiation or TL measurement. This not only re-establishes the defect equilibrium within the material but also empties the deep traps that act as competitors. Since fluorite is a natural mineral and is highly sensitive to radiation, it contains a natural TL response. This natural TL makes the sensitivity of fluorite phosphor highly variable with respect to dosimetric features owing to the presence of unstable traps. To get reproducible results, high-temperature annealing was thus essential [29, 33]. In literature, different regimes were available for annealing the natural TL (from 400 ^{o}C to 650 ^{o}C in air for different time durations), but a comprehensive study was necessary for these local materials to be used as radiation dosimeters [11]. Therefore, annealing at 500 °C for 2 hours was determined feasible for natural TL removal and the reproducibility of the phosphor TL. The thermal treatments were performed by a programmable Nabertherm-P330 furnace.

2.4 Self-Dose Assessment

Since fluorite is a natural mineral, the studied sample may contain some Naturally Occurring Radioactive Material (NORM). This can be problematic when the material is stored over some time i.e. for the TL fading studies or used as an environmental dosimeter. To check the self-dose of the natural fluorite, the assessment of NORMs was made with a HPGe detector Model: GC-3020 and the dedicated software Genie 2000 version 2.1 (Canberra, USA), available at Environmental Monitoring Group (EMG), Pakistan Institute of Nuclear Science and Technology (PINSTECH), Islamabad, Pakistan. The counting was performed for a period of 18 hours (≈ 65000 s) taking a weight of 100 grams in a Marinelli beaker as mentioned by Ghias *et al.* [34]. The procedure performed is mostly used for the assessment of radioactivity from environmental samples.

2.5 Luminescence measurement facilities

All TL measurements were carried out with an automated Risø TL/OSL reader [35]. Unless stated otherwise, the glow curves were recorded from 40 to 400 °C at a heating rate of 2 °C /s under a nitrogen atmosphere. The signals were detected in the UV using 7.5 mm Hoya U-340 filters in front of the bi-alkali photomultiplier tube PDM 9107Q-AP-TTL-03 (160–630 nm) [36]. Irradiation was performed using a ^{90}Sr/^{90}Y beta source (Max. 2.28 MeV) having dose rate of 4.8 Gy/min, mounted on the reader, which was calibrated at for sand-sized quartz on stainless steel discs [36]. For measurement, a monolayer of approximately 1 mg of fluorite grains was mounted on the inner 2 mm of the stainless steel discs using silicone oil as an adhesive.

The net TL signal was obtained by subtracting the background observed during a second heating of the same aliquot from the glow curve. For the majority of the measurements, the average TL intensity from at least two aliquots was used.

3 Results and Discussion

3.1 Thermoluminescence glow curve structure

The integrated response or electronic charge collected by the PMT versus time or temperature is termed the glow curve of the sample under observation. Figure 2 shows the TL response to a regenerative dose of 0.8 Gy for the seven natural fluorite samples. All the glow curves and analyses were average responses per unit mass.

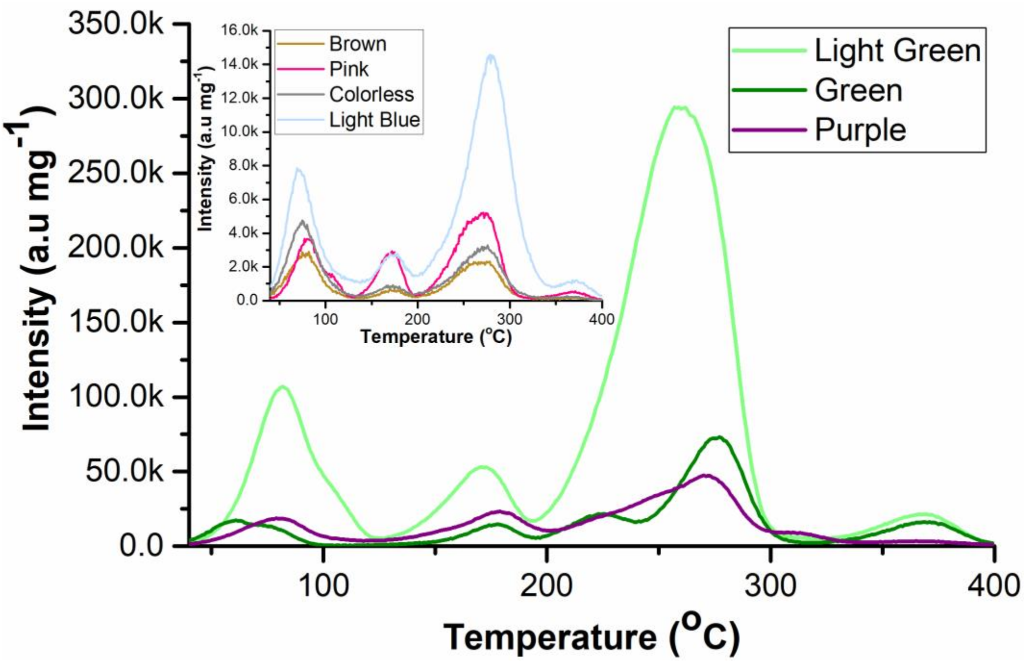

Figure 2: TL glow curves of the seven fluorite samples with different colors

All the fluorite samples exhibit a composite glow curve structure with different peak positions and the same number of broad peaks. These variations (as discussed earlier in Section-I) may be correlated to the type and concentration of impurity atoms present in different fluorite colors. Numerous scientists have investigated the TL properties of regional fluorites. Sohrabi *et al*. has investigated TL responses of nine batches from different mines of Iran [37]. Balogun, *et al*. discussed the low temperature peaks up to 250 ^{o}C of purple fluorite from Nigeria [21]. Topaksu, Yegingil, and Atlihan have studied various TL properties of colorless, light green, green and blue fluorites from Turkey respectively [10, 11, 38]. These studies on fluorite samples showed differences in glow curve structure with variations in peak height and area. It was also suggested that green and light green fluorites produce the most intense glow peaks.

3.2 Selection of sample

The light green (LG) variant showed the highest luminescence sensitivity, measured as response per unit mass per unit dose, of the seven fluorite samples from Pakistan examined, while the brown one has the lowest. Also, the percentage of the peak's area near 250 ^{o}C compared to complete glow curve of LG fluorite was the highest of all the samples and may be suitable for dosimetric purposes. Also, no significant number of counts greater than the background was obtained when subjected to self-dose assessment. Therefore, it was concluded that there is no significant dose due to internal radioactivity present in the LG fluorite sample. Considering the aforementioned observations, LG fluorite sample was selected for chemical and mineralogical characterization, and further TL dosimetric and kinetic analysis.

3.3 Structural, morphological, and chemical analysis of the selected sample

The peaks of the XRD pattern of LG fluorite were well-matched with the peaks of ICDD card no. 00-004-0864 and one of the diffraction pattern of the LG Fluorite is shown in Figure 3.

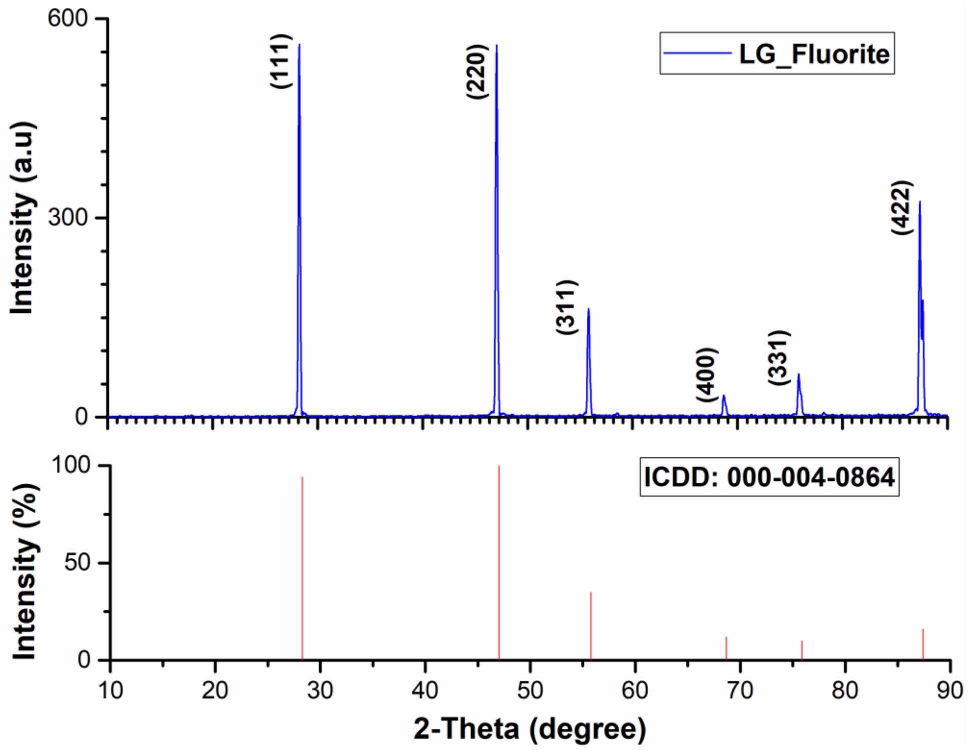

Figure 3: XRD diffraction pattern of LG Fluorite and the matched ICDD database card no. 00-004-0864

Fluorite has a face-centered cubic (FCC) crystal system and the related data are given in Table 1. The strong and sharp diffraction peaks confirm the presence of LG fluorite and the absence of any other crystalline material. Using the data in Table 1 and equation (1), the average crystallite size was calculated to be 43 nm, which is much smaller than the particle size used in this study.

Table 1: Structural, crystallographic, and h, k, l parameters of the light green fluorite

Name	Chemical Formula	Crystal System	Space Group	Z	
Fluorite	CaF_2	Cubic (FCC)	Fm3m	4	
Crystallographic parameters					
a(Å)	**b(Å)**	**c(Å)**	**α(o)**	**β(o)**	**γ(o)**
5.4626	5.4626	5.4626	90	90	90
2 (theta)		**FWHM [°2Th.]**	**d-spacing (Å)**	**hkl**	
28.2655		0.2755	3.15738	111	
47.0798		0.2362	1.93030	220	
55.7264		0.2362	1.64955	311	
68.6263		0.2165	1.36760	400	
75.7989		0.1968	1.25503	331	
87.3494		0.1968	1.11639	422	

The results from the elemental analysis of the LG fluorite sample using Inductively Coupled Plasma Optical Emission Spectrometry (ICP-OES) are listed in Table 2. The ICP-OES analysis reveals the presence of 93.82% of light green fluorite with the main impurity being quartz or silica (4.93%). The detection of rare earth impurities does not fall within the scope of this study.

Table 2: Major and trace elements present in the light green fluorite

Element	**Ca**	**F**	**Al**	**B**	**Cu**	**Fe**	**K**	**Mg**	**Na**	**Si**
Content (%)	76.29	18.61	0.24	0.87	0.05	0.05	0.01	0.01	0.29	3.86

EDS analysis provides the major elements of CaF_2 sample as shown in Figure 4 (a). The maximum intensity of calcium (34.14%) and fluorine (47.45%) in the spectrum indicates the high concentration of CaF_2 as depicted by ICP-OES results. The surface morphology of the powder sample (Figure 4 (b)) shows that it has irregular shape particles of different sizes between 63 to 180 µm.

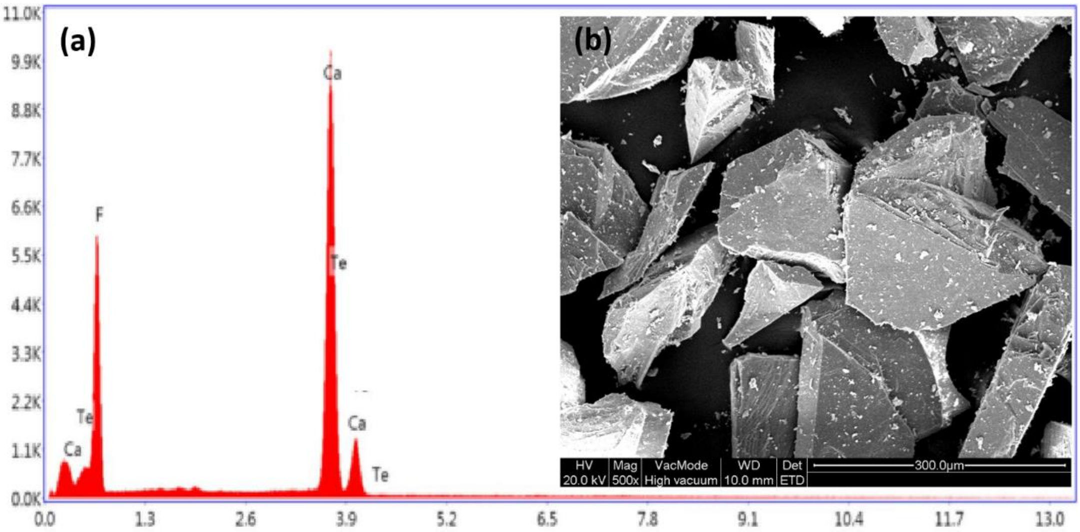

Figure 4: (a) EDS analysis and (b) SEM image of the LG Fluorite

3.4 Dose response

Figure 5 shows the TL glow curve structure of the LG fluorite at a heating rate of 1 °C/s after exposure to β-radiation for different times. The glow curve is a composite one having five visible peaks at about 75, 100, 163, 251, and 358 °C. Sunta *et al.* and Chougaonkar and Bhatt have attributed these peaks to the reduction-oxidation process of REEs like Ce, Gd and Dy, from +3 to +2 and vice versa, especially the 251 °C peak with Ce^{+3} [39, 40]. The favorable concentration of Ce^{+3} atoms in LG fluorite could be responsible for good TL response as compared to other six samples. The resulting TL emission is in the 320 – 340 nm wavelength range which is preferred by most of the PMTs in TLD readers.

The area under peaks# 1and 2 combined (further denoted as the Low-Temperature Peak, LTP), peak# 3, peak# 4 (further termed as the Dosimetric Peak, DP), and peak# 5 is approximately 15%, 7%, 73%, and 5% respectively. The peak areas are almost the same as reported by Schayes *et al*. [17]. The percentage area of each peak remains almost constant in the studied dose range of 80-5120 mGy. This suggests that DP together with peak# 3, covering 80% relative peaks area of total and being at reasonably high temperatures, can be used for dosimetry. The LTP is not useful for this application because the low temperatures peaks are thermally unstable. Peak#5 looks unsuitable because of its low intensity and is at very high temperatures. The broadness and the shape of the DP elucidates that it may be a composite one. This is discussed in detail in Section 3.8.

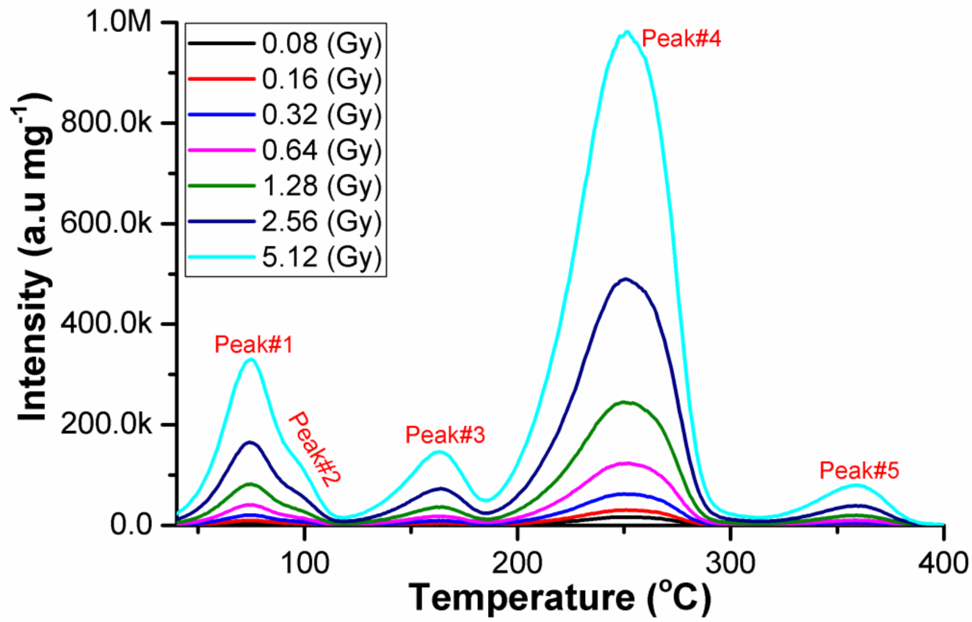

Figure 5: TL glow curves of the LG Fluorite at a heating rate of 1 °C/s, after different *β* exposures (dose rate = 4.8 Gy/min)

Compared to the structure and the response of light green fluorite from Turkey studied by Yegingil *et al*. [11], the percent area of the principal dosimetric peak (DP) of the Pakistani fluorite is approximately 20-30 % more with the presence of an additional peak (peak#5) in the glow curve.

Figure 6 shows the dose-response curves when taking the complete glow curve as well as the individual peaks. At a particular dose value, each point on the dose-response curves indicate the variation in the area of the respective peak with respect to the whole glow curve.

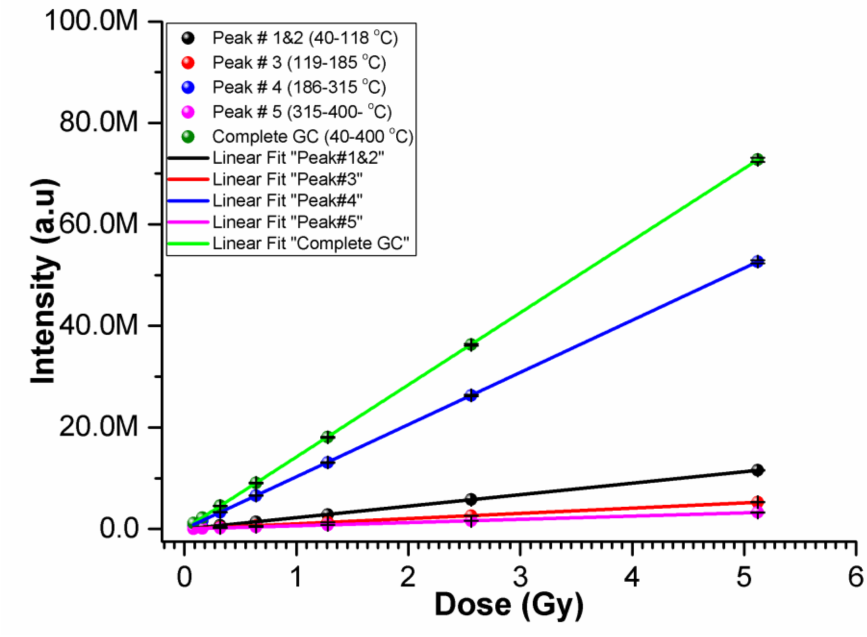

Figure 6:Dose responses of the complete glow curve and the individual peaks. The solid lines represent the linear fit (y=a +b*x) to the data.

Table 3 shows the fitting parameters of the dose-response curves of the individual and the complete GC when the linear fit is applied. The value of Adj. R-square = 1, shows the best fitting for the main dosimetric peak, DP.

Table 3: Fitting parameters of the dose-response curves of LG Fluorite

Peak #	Intercept	Standard Error	Slope	Standard Error	Adj. R-Square
1&2	-20431	8388	2261550	3754	0.99998
3	-5799	4480	1029680	2005	0.99998
4	5076	18745	10267200	671	1
5	-1301	6850	636062	3065	0.99986
Complete GC	-22620	30690	14204200	13734	0.99999

Many factors affect the TLD responses but heat treatment and dose variation are the most significant. The dose-response of fluorite can be best understood by the dose linearity index function *F(D),* which is defined as the ratio of normalized dose-response and is given by the following formula (2) [41]:

$$F(D) = \frac{TL_{response}(D)/D}{TL_{response}(D'')/D''} \qquad (2)$$

Where *TL* $_{response}$ *(D)* is the material response at various doses (here in between 80 - 5120 mGy) and *TL*$_{resp}$ *(D'')* is the response at the lowest possible dose (80 mGy in this case) at which it shows linear behavior. Based on the value of *F(D),* the response of a TLD phosphor is designated as linear, sub-linear and supra-linear for *F(D)* =1, *F(D)* < 1 and *F(D)* > 1 respectively. Figure 7 shows the plot of the linearity index function with a dose for LG fluorite. Figure 7 demonstrates that LG fluorite shows a linear dose-response, within the experimental uncertainty for the examined dose range.

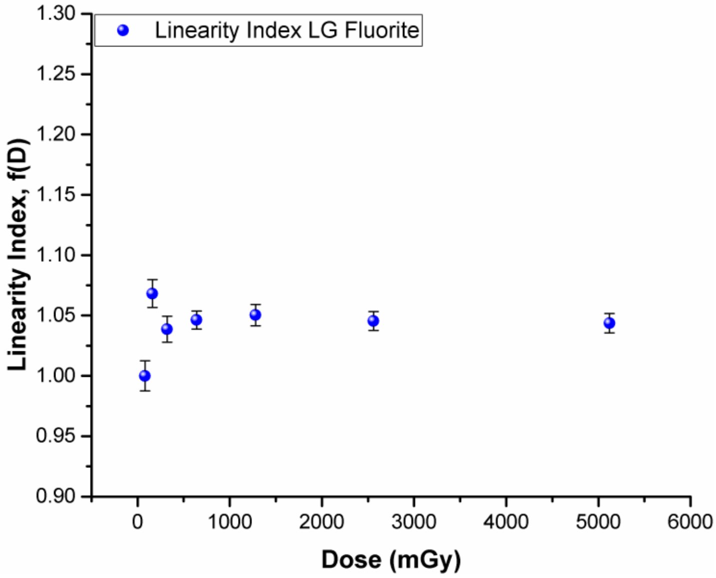

Figure 7:Variation in the linearity index value of LG fluorite with respect to dose

3.5 TL Sensitivity

The sensitivity of a TL material can be defined as the TLD response in reader units, per unit dose, per unit mass. It is very difficult to determine the absolute sensitivity of a TLD due to the variations in readout systems. However relative sensitivity can be evaluated if the TLD signal is compared with the TL signal from some standard TLD such as CaF_2: Dy (TLD-200) keeping the other factors same i.e. dose and mass. The relative sensitivity is measured after irradiating both, the TLD-200 chips and LG fluorite to a 1000 mGy dose. The average of five readouts is taken for both TLDs for relative sensitivity calculation. The sensitivity of LG fluorite is found to be 26 times higher than the TLD-200.

3.6 Minimum Detectable Dose (MDD)

In the field of dosimetry, the sensitivity and the minimum detectable dose (MDD) of any phosphor are very important properties of the phosphor. Fluorite is also well known for its maximum sensitivity and low MDD values. Literature shows that to obtain a low detection limit, a combination of a high sensitive dosimeter with a photomultiplier tube having maximum efficiency in the spectral range of the TL emission is essentially required [42]. The MDD is calculated using the following expression,

$$MDD(TL) = \left(\overline{m}_{Background} + 2\sigma_{Background}\right) * c.f \qquad (3)$$

Where $\overline{m}_{Background}$ is the mean of the background responses obtained from 10 un-irradiated samples, $\sigma_{Background}$ is the standard deviation obtained from the background signal and *c.f* is the calibration factor defined in terms of mGy/TL response derived from the fitted data of dose response curve (Table 3).

An *MDD(TL)* of 9.7 mGy is calculated using equation (3) when response of complete GC is taken. The determined MDD value can be much lower than this. The high MDD value as compared to commercial TLDs (≈ 10 μGy) could be owing to the high residual signal and the high number of background counts due to the thermionic emission in the measured temperature range [43]. This can be minimized by considering proper time-temperature profiles and annealing conditions taking into account the previous irradiation history [44, 45].

3.7 Repeatability

The TL sensitivity (response per unit dose) of a TL material may change on repeated use (e.g. multiple cycles of irradiation, annealing and readout). This can be due to the depletion or the creation of some traps and/or the change in the concentration of charge carriers in deep, competing traps within the dose range understudy. When a TL material is to be used for dosimetry, it must be subjected to a repeatability test to ensure that it has the same response during each reuse process. The LG fluorite was tested for its repeatability by repeating multiple identical cycles of heating and irradiation (using a dose of 0.56 Gy, recording the glow curve up to 400 ^{o}C at a heating rate of 1 ^{o}C/s and second readout for background and annealing process). The responses for all cycles (inset Figure 8) are normalized to the mean of all the readings. A progressive decrease of maximum 0.5% per cycle is observed in the response which reached to about 4% after 10 cycles of irradiation, readout and annealing. The coefficient of variation (COV%) as determined according to the procedure given by Furetta [44] is less than 1%. Figure 8 also demonstrates that the glow curve structure of LG fluorite does not change significantly after many applications. This indicates that it is suitable for dosimetric applications.

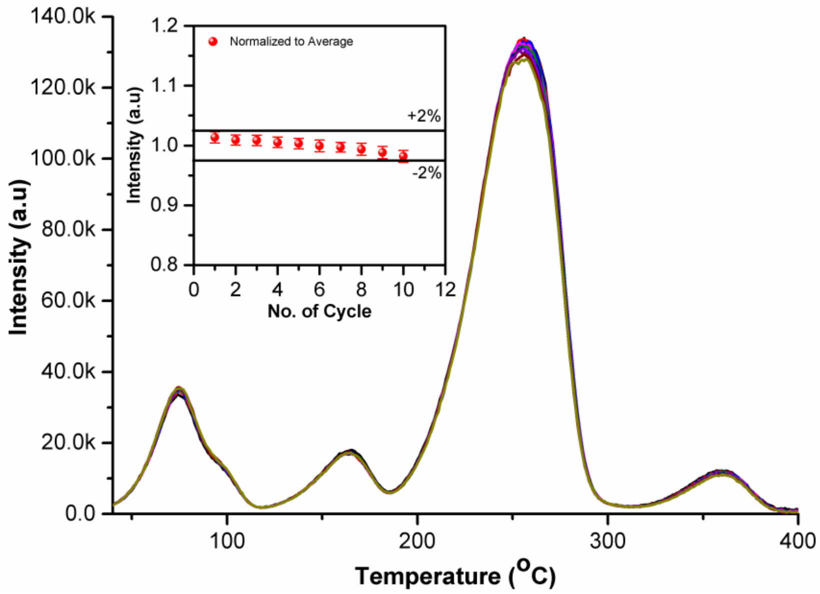

Figure 8: Repeated GCs of the LG fluorite after 10 cycles of irradiation, readout, and annealing. The inset shows the response variation (considering the entire glow curve) with respect to an average of all readings.

3.8 Fading

Fading study of the TL signal with time is an important parameter of TL dosimeters whether they are used for personal or environmental dosimetry. The stability of the signal in the operational environments may be compromised by heat (thermal fading), light (optical fading), or by any other internal mechanism (anomalous fading). It is, therefore, desirable for dosimeters that their glow peak temperature should be around 200 to 250 ^{o}C to evade thermal fading [7]. This fading will be higher for peaks with shallow traps while very small or approximately no fading will be observed for deep traps i.e. $E > kT$.

To assess that the loss of TL signal is only due to thermal decay, a fading experiment has been performed by repeatedly measuring the response to 0.56 Gy regenerative dose following different storage times at ambient room temperature up to approximately one month. All the measurement values are normalized to the first reading taken just after the irradiation. Figure 9 shows the fading characteristics of the TL signal of the LG fluorite. The maximum fading of the integrated signal (the whole GC) is due to LTP. About 2% of the total signal of which 1.2% is from LTP fades in 2.4 hours. It takes about a week for LTP to completely fade from the glow curve signal and after that it remains almost constant. About 5% of the signal decays during the first 24 hours which reaches up to 8% in approximately one month. Comparing the results with the fading studies by Sohrabi et al., Latif et al., and Yegingil et al. [11, 37, 46], the small percentage of fading of integrated signal is because of the smaller percentage area of the LTP as compared to rest of the peaks including DP. For more detailed results, a fading study for individual peaks with post-irradiation annealing can be conducted.

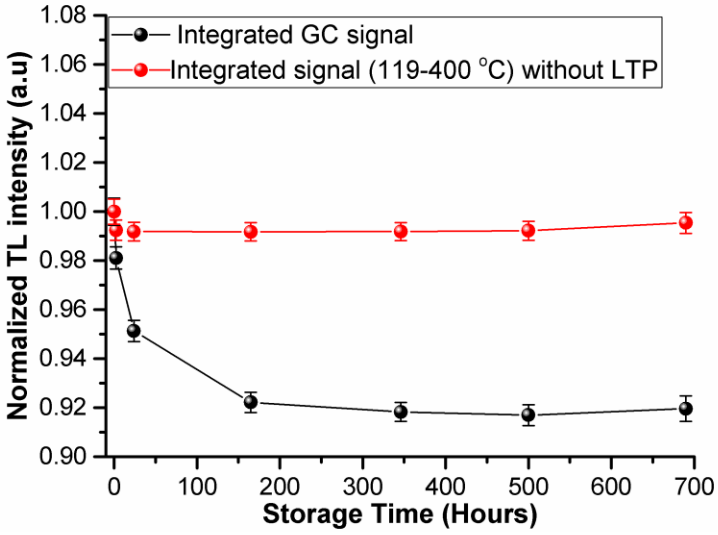

Figure 9: Signal loss as a function of storage time after irradiation.

3.9 Kinetic parameters and lifetime analysis

The physical characteristic of a glow curve such as the peak position (the temperature of the peak maximum, T_m) and the area covered by the peak, as discussed in earlier sections, can be linked to the type and concentration of traps created by impurity atoms. It also depends on the thermal and other conditions during formation of the TL material. The key parameters of the traps thus formed in any TL material include the activation energy (E) of the trapped charge carriers and the frequency factor (s). Additive Dose (A.D), T_m-T_{stop}, Computerized Glow Curve Deconvolution (CGCD) and Various Heating Rate (VHR) methods are used for the determination of these parameters. The other parameters like the order of kinetics (b), the peak maximum temperature (T_m), and subsequently the lifetime (τ) of the traps are beneficial in understanding the charge transfer processes taking place in the material, which are ultimately responsible for the generation of TL [7].

3.9.1 Additive Dose (A.D.)

The first step suggested in the analysis of GC or estimation of kinetic parameters is to find the value of "b" [3, 44]. The easiest way of estimating the value of "b" is the Additive Dose (*A.D.*) method. A.J.J. Bos has shown that for first-order kinetics (FOK) i.e. b=1, the temperature of the peak maximum (T_m) is independent of the initial concentration of charge carriers n_o (concentration of trapped charge carriers $n_o > N$ concentration of traps) which is proportional to the dose absorbed [5]. It means that if T_m does not change with dose variation it should be assigned b=1. For $1< b \leq 2$, the T_m shifts to the lower temperature on increasing the dose level and vice versa (thermal cleaning). The estimated value of E using T_m can be approximated by the method described by C.M. Sunta [3]. As expected for FOK (i.e., b=1), the T_m of the peaks does not shift more than the experimental margin of ±3°C (Figure 5).

3.9.2 T_m-T_{stop}

After estimating “b” one should go with the methods which are independent of the shape of the glow curve, because the neighboring weak satellite peaks in the experimental glow curve may produce uncertainties in the values of kinetic parameters. T_m-T_{stop} and the Repetitive Initial Rise (RIR) methods help estimate the number of individual peaks including any satellite peaks with T_m and their activation energies respectively [47-49]. McKeever (1980) proposed that the T_m-T_{stop} method not only assists in locating the peak position, but also provides the information about trap distribution associated with each peak i.e. localized or continuous. In this procedure, the TLD sample is irradiated to a fixed low dose. The sample is then linearly heated to some point (T_{stop}) on the low-temperature tail of the very first peak. Once cooled to room temperature, the remaining glow curve is recorded under the same conditions and the temperature of the maximum intensity (T_m) of the very first peak in glow curve is determined. The complete process is repeated with small increments in T_{stop} (usually between 2 to 5 °C). A plot of T_m versus T_{stop} is then made.

If it shows a well-defined staircase shape and sharp rise at the end of each step, this indicates the presence of well-separated peaks (presence of FOK) in the glow curve with the discrete distribution of traps. The number of steps corresponds to the total number of peaks and b=1.

The glow curves are obtained with a heating rate of 2 °C/s and a dose of 800 mGy. A temperature increment of 3°C is used for T_{stop} and the corresponding T_m value is noted. Figure 10(a) shows the T_m-T_{stop} plot for the investigated sample of LG fluorite. The plateau regions formed in the plot show that the glow curve of the LG fluorite is a composite one with six individual overlapping peaks at about 82, 104, 172, 265, 272 and 371 °C. From the shape of the staircase pattern, it can be inferred that the peaks follow FOK i.e. b=1 as found by the fluorite from Turkey [11]. This information is used in the CGCD method for the determination of kinetic parameters as discussed in the next section. The same glow curves can be exploited to determine the activation energies of the individual traps using Initial Rise (IR) method, also called Repetitive Initial Rise (RIR) method [50, 51]. Taking the initial rising part (up to 15% of the peak maximum height) of the glow peak in which the concentration of trapped charge carriers i.e. $n(T)$ remains almost constant, the TL intensity can be expressed as $I\ (T) = c\ \exp\ (-E/kT)$. The slope of the straight line obtained by plotting $ln(I)$ vs $1/kT$, yields the activation energy (E) against each T_{stop}. From the plot of E vs T_{stop} as shown in figure 10(b), the obtained activation energies were 1.07±0.03, 0.83±0.04, 1.20±0.2, 1.53±0.04, 1.43±0.05, 2.19±0.08.

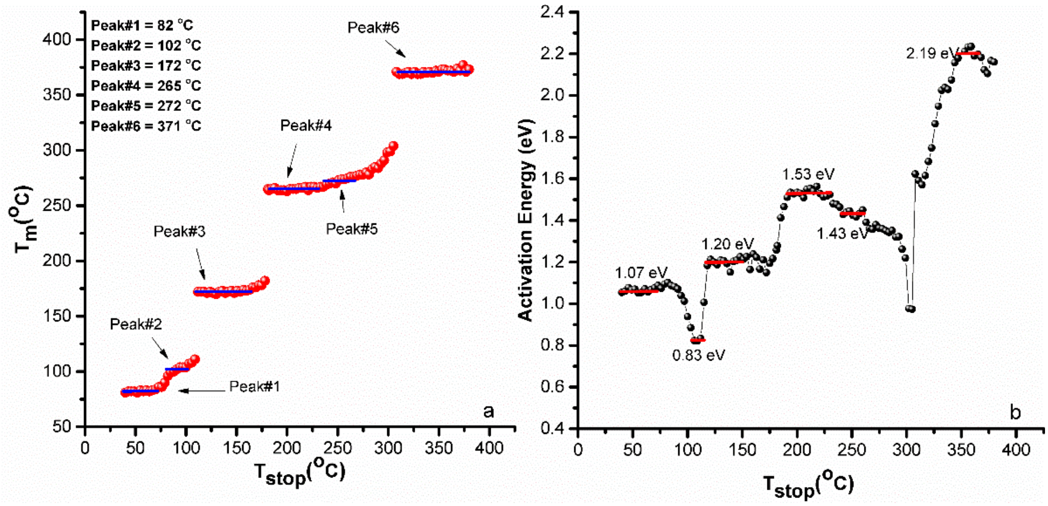

Figure 10: (a)T_m-T_{stop} plot of LG fluorite. The legend shows the number and temperatures of peak maximum (T_m). (b)Activation energy vs T_{stop} plot of LG fluorite showing E (eV) of each trap

3.9.3 Computerized Glow Curve Deconvolution (CGCD)

Better results are produced if the kinetic parameters of individual peaks are estimated using computerized glow curve deconvolution (CGCD) in combination with the T_m-T_{stop} method. The exact number of individual peaks helps in the deconvolution of the complex glow curve structure of the phosphor. CGCD has become an essential method for TL glow curve analysis due to its practical benefits, not only in the estimation of kinetic parameters but also in TL dosimetry [52, 53]. The newly developed and freely available Microsoft Excel-based program “GCD Analyzer” has been employed to investigate the fitted peaks parameter [54]. The findings of *A.D.* and T_m-T_{stop} procedures i.e. FOK (i.e. b=1) and six number of individual peaks are set as parameters of the program. The fitted peaks are generated using the rational approximation into the first order kinetic model of Randall–Wilkins [55]. To avoid the variations due to the applied dose and the other conditions, the deconvolution is done on the glow curves obtained under the same conditions at which the T_m-T_{stop} procedure is used. Figure 11 shows the graph of the CGCD analysis. The goodness of the fitting processes is assessed by the Figure Of Merit (*F.O.M*) suggested by Balian and Eddy [56].

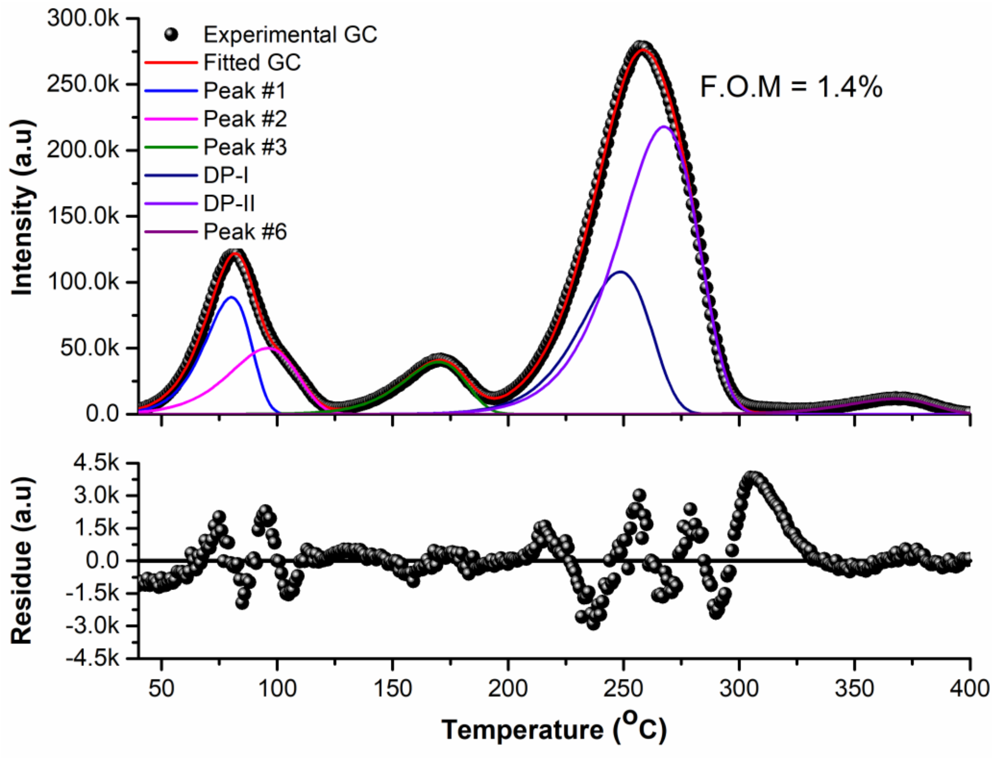

Figure 11: Results from CGCD analyses. The residual displays the unfitted areas in the glow curve

The kinetic parameters obtained after CGCD analysis are listed in Table 4. A *F.O.M* of 1.4% is obtained. The T_m of most of the peaks is the same as obtained in the T_m-T_{stop} except peak# 2, peak# 4 (DP-I), and peak#5 (DP-II) (see Table 4). One of the reasons for the difference in results can be the high overlapping regions present between the individual peaks. The other reason may be the presence of some low-intensity satellite peaks which are imperceptible in the T_m-T_{stop} process and indicated by the residual of the fitting process in Figure 11. The small differences in T_m of peak# 1, peak# 3 and peak# 6 may be the fact that the results from T_m-T_{stop} are sensitive to where exactly one defines the plateau-regions.

Table 4: Kinetic parameters of the traps obtained after deconvolution of TL glow curve

Peak No.	Peak Temperature T_m (°C)		Trap Depth E (eV)	Frequency Factor s (s^{-1})	Life Time τ (y)
	T_m-T_{stop}	CGCD			
1	82	81	1.06 ± 0.04	2.82×10^{14}	1.05×10^{-4}
2	104	97	0.78 ± 0.05	5.84×10^{9}	8.18×10^{-5}
3	172	171	1.22 ± 0.02	1.13×10^{13}	1.27×10^{0}
DP-I	265	250	1.51 ± 0.03	5.14×10^{13}	$2.25 \times 10^{+4}$
DP-II	272	268	1.44 ± 0.04	2.94×10^{12}	$2.29 \times 10^{+4}$
6	371	369	1.90 ± 0.02	1.01×10^{14}	$5.00 \times 10^{+10}$

3.9.4 Approximation approach

In the TL process, a well-known key parameter of glow curve is the peak position T_m which is related to E (for FOK) by the equation (4) as,

$$\frac{s}{\beta} = \frac{E}{kT_m^2} \, exp\left(\frac{E}{kT_m}\right) \quad (4)$$

Using approximation rule discussed by Sunta (2014) [3], instead of dealing with fitted peak#4 and peak#5 (due to very close values of trap depths), one can consider the combined peak called the dosimetric peak (i.e. DP) for the determination of kinetic parameters. The effective trap depth (E_{eff}) of the DP taken as the average of the constituent peaks DP-I and DP-II is 1.48 eV. The approximation approach yields a numerical solution of equation (4) for various combinations of E and s/β given by a linear relationship as

$$E = aT_m^c \quad (5)$$

where a and c are constants and β is the linear heating rate. For $s/\beta = 0.5 \text{ x } 10^{13}$ (assuming s equal to Debye frequency i.e. 10^{13} s^{-1} and $\beta = 2$ °C/s) the approximate value of the E for DP ($T_m = 259$ °C) turns out to be 1.45 eV. The values of kinetic parameters for other peaks are given in Table 5. The values of E and s obtained by CGCD and the approximation approach are in close agreement.

3.9.5 Various Heating Rates (VHR)

In this section, kinetic parameters are determined using an experimental method like Various Heating Rates (VHR) and later, a comparison is presented with the estimated values obtained through CGCD method. The change in T_m with the change in heating rate has been reported to find the kinetic parameters of the glow peaks. Figure 12 shows the GC of LG fluorite obtained with a constant dose of 0.8 Gy and heating rates of 0.1, 0.5, 1, 3, 7, and 10 °C/s.[3]

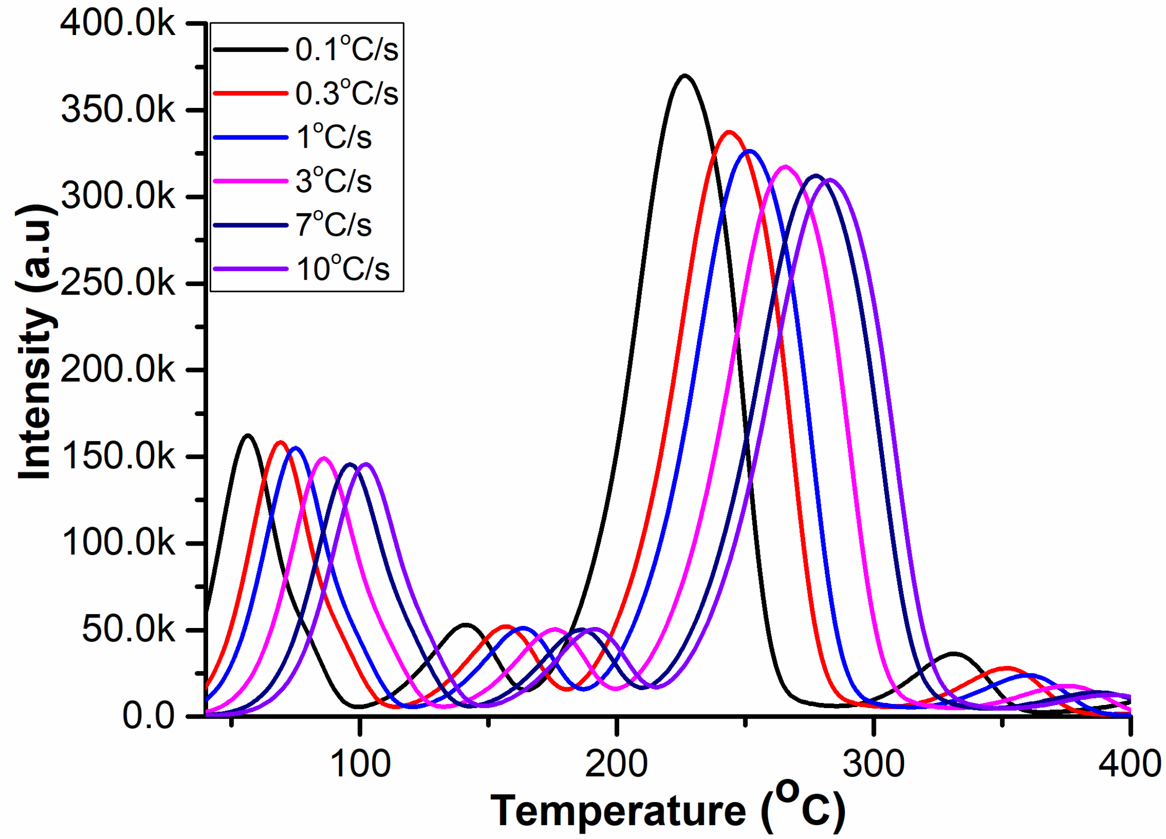

Figure 12: Glow curves of LG fluorite after different heating rates

One way of using *VHR* (designated as *Method-I*) is to use the numerical values of different heating rates in combination with their respective T_m. For FOK, Sunta showed that if one can measure T_m with an accuracy of 1 %, the value of E can be calculated with an accuracy of about 5 % [3]. For any two different heating rates β_1 and β_2 (with corresponding peak maximum temperatures T_{m1} and T_{m2}) in equation (4) and eliminating s, the following expression is obtained for the calculation of the trap depth (E) [44].

$$E = \left[\frac{kT_{m1}T_{m2}}{T_{m1}-T_{m2}}\right] ln \left[\left(\frac{\beta_1}{\beta_2}\right)\left(\frac{T_{m2}}{T_{m1}}\right)^2\right] \qquad (6)$$

The frequency factor s can be calculated by substituting the numerical value of E in equation (4). The other, rather graphical method (designated as *Method-II*) is suggested by Hoogenstraaten *et al*. [57]. Plotting $ln(T_m^2/\beta)$ verses $1/T_m$ for different heating rates, one gets a straight line of the slope (E/k) and intercept ln (sk/E). The values of slope and intercept are used to get E and s. The value of s can also be calculated using equation (4). Figure 13 shows the fitted lines and the respective data of slope and intercept for the calculation of kinetic parameters.

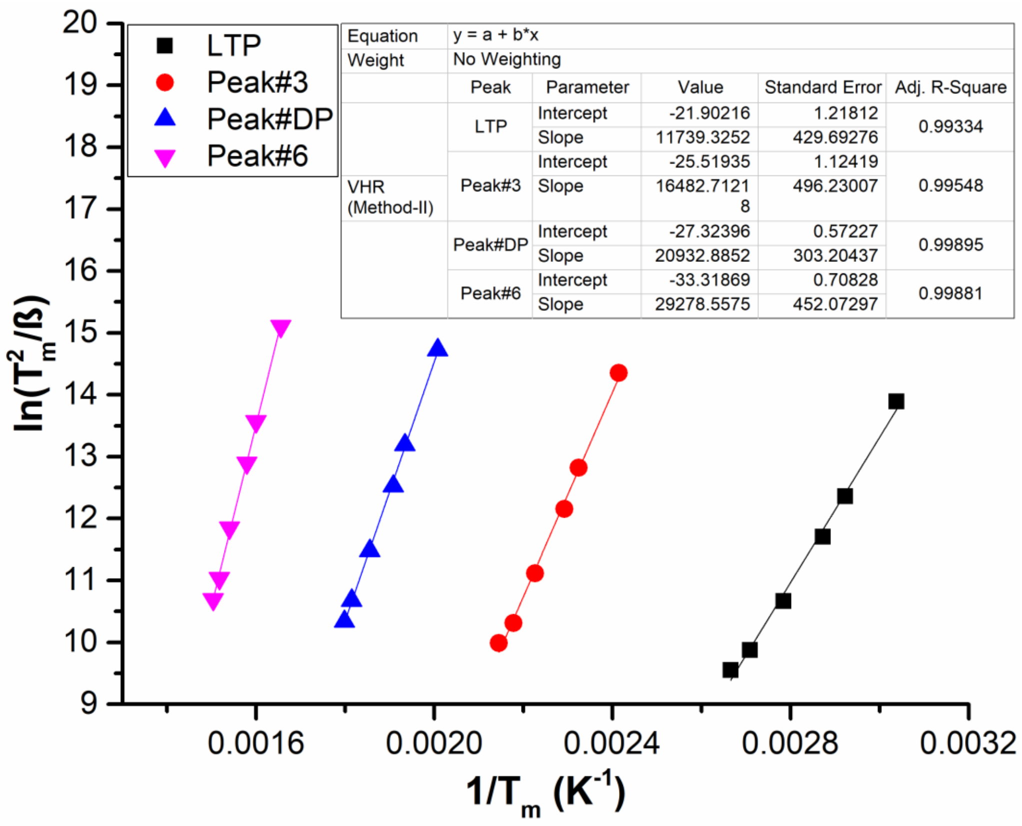

Equation	y = a + b*x				
Weight	No Weighting				
	Peak	Parameter	Value	Standard Error	Adj. R-Square
VHR (Method-II)	LTP	Intercept	-21.90216	1.21812	0.99334
		Slope	11739.3252	429.69276	
	Peak#3	Intercept	-25.51935	1.12419	0.99548
		Slope	16482.71218	496.23007	
	Peak#DP	Intercept	-27.32396	0.57227	0.99895
		Slope	20932.8852	303.20437	
	Peak#6	Intercept	-33.31869	0.70828	0.99881
		Slope	29278.5575	452.07297	

Figure 13: Graph of VHR (Method-II) showing the line plots and the extracted data (inset table) for the calculation of kinetic parameters

Table 5 shows a comparison of the kinetic parameters calculated using *CGCD*, *approximation* and the above-discussed two different methods of *VHR*. Due to highly overlapping nature of the individual peaks in LTP (Peak#1 and peak#2) and DP (DP-I and DP-II), the kinetic parameters are determined using the T_m of the composite peak.

Table 5: Comparison of the kinetic parameters obtained by CGCD, approximation and the two methods of VHR. LTP (Peak# 1 and Peak# 2) and DP (DP-I and DP-II) are the two composite peaks

Peak		CGCD		Approximation		VHR (Method-I)		VHR (Method-II)	
		E (eV)	s (s^{-1})	E (eV)	s (s^{-1})	E (eV)	s (s^{-1})	E (eV)	s (s^{-1})
LTP	Peak#1	1.06 ±0.04	2.82 x10^{14}	1.08 ±0.06	1.00 x10^{15}	0.97 ±0.05	1.24 x10^{15}	1.01 ±0.06	1.01 x10^{13}
	Peak#2	0.78 ±0.05	5.84 x10^{9}						
Peak#3		1.22 ±0.02	1.13 x10^{13}	1.28 ±0.04	1.00 x10^{14}	1.38 ±0.03	1.15 x10^{19}	1.42 ±0.04	1.99 x10^{15}
DP	DP-I	1.51 ±0.03	5.14 x10^{13}	1.45 ±0.05	1.00 x10^{13}	1.84 ±0.04	4.47 x10^{19}	1.80 ±0.03	1.54 x10^{16}
	DP-II	1.44 ±0.04	2.94 x10^{12}						
Peak#5		1.90 ±0.02	1.01 x10^{14}	1.88 ±0.04	1.00 x10^{14}	2.54 ±0.03	1.27 x10^{22}	2.52 ±0.05	8.65 x10^{18}

The value of *E* estimated by the two methods of *VHR* are very close to each other, but the values of *s* is a bit higher than calculated by *Method-II*. The values of both E and s estimated by *VHR* methods are on higher side compared to the ones obtained by CGCD and approximation methods. One of the reasons for these higher values may be the inaccuracies in finding the T_m of the individual peaks with reasonable accuracy and the temperature lag during measurements at higher heating rates.

3.9.6 Effect of dose variation on the kinetic parameters

To study the effect of dose on the kinetic parameters, the glow curves of LG fluorite, recorded at a heating rate of 1°C/s with doses of 0.32, 1.28, 2.56 and 5.12 Gy, are de-convolved using CGCD and the results are presented in Table 6. The value of trap depth for DP-II is decreased by a maximum of 0.1 eV at higher doses. There is a difference of around 2 K between the peak maximum temperatures (T_m) of individual peaks at the specified doses. These small variations with dose suggest that the constituent peaks of the TL glow of LG fluorite follow FOK. The little higher values at 0.32 Gy compared to other doses and the decrease in F.O.M with increased dose as shown in Table 6, suggest that the deconvolution process should be performed at some suitable high doses (of the order of Grays).

Table 6: Kinetic parameters and FOM of the fitted glow curves at different doses

Dose (Gy)	**Peak No.**	**Peak max. Intensity (I_m)**	**Peak Temperature T_m (K)**	**Trap Depth E (eV)**	**Frequency Factor s (s^{-1})**	**F.O.M (%)**
0.32	**1**	14686	347.3	1.06 ± 0.03	2.6 x 10^{+14}	1.75
	2	9198	363.9	0.78 ± 0.04	4.1 x 10^{+09}	
	3	8636	436.4	1.20 ± 0.03	5.7 x 10^{+12}	
	DP-I	31036	513.4	1.34 ± 0.04	8.3 x 10^{+11}	
	DP-II	49494	536.3	1.60 ± 0.05	6.4 x 10^{+13}	
	5	4966	633.1	2.05 ± 0.04	1.3 x 10^{+15}	
1.28	**1**	57864	346.1	1.05 ± 0.03	1.9 x 10^{+14}	1.72
	2	37435	362.4	0.76 ± 0.04	2.6 x 10^{+09}	
	3	34195	435.4	1.19 ± 0.02	4.3 x 10^{+12}	
	DP-I	125980	512.7	1.33 ± 0.03	7.5 x 10^{+11}	
	DP-II	192442	535.6	1.61 ± 0.04	9.3 x 10^{+13}	
	5	19471	640.9	2.06 ± 0.03	1.5 x 10^{+15}	
2.56	**1**	115621	346.1	1.05 ± 0.04	1.8 x 10^{+14}	1.62
	2	76258	362.3	0.75 ± 0.03	1.9 x 10^{+09}	
	3	68053	435.6	1.19 ± 0.02	4.1 x 10^{+12}	
	DP-I	213905	511.6	1.34 ± 0.03	9.7 x 10^{+11}	
	DP-II	407615	534.4	1.51 ± 0.06	1.1 x 10^{+13}	
	5	38600	632.1	2.06 ± 0.03	1.7 x 10^{+15}	
5.12	**1**	234476	346.0	1.04 ± 0.03	1.4 x 10^{+14}	1.56
	2	149823	362.4	0.76 ± 0.04	2.7 x 10^{+09}	
	3	137512	435.2	1.18 ± 0.03	3.7 x 10^{+12}	
	DP-I	432668	510.9	1.34 ± 0.04	9.3 x 10^{+11}	

DP-II	822353	534.0	1.53 ± 0.05	1.7 x 10^{+13}
5	78520	631.8	2.04 ± 0.04	1.1 x 10^{+15}

3.9.7 Lifetime

The main purpose of calculating these kinetic parameters i.e. E, s and b is to look inside the physical processes taking place in the phosphor such as fading. Thermal fading at room temperature can be understood from the lifetime (τ) of trapped electrons calculated using equation (7) at T=25°C (298 K).

$$\tau = s^{-1}\, exp\left(\frac{E}{kT}\right) \tag{7}$$

Where k is Boltzmann's constant. The values of τ are calculated by taking the values of E and s determined using CGCD method and given in Table 4. The calculated lifetimes (often not representing the true fading time) are compared with the actual fading time. The life times of both peak#1 and 2 are around 1 hour while it takes about one week to completely vanish them from the glow curve. Comparison of other peaks is little hard due to their slow fading and long life times.

4 CONCLUSIONS

Pakistani natural calcium fluoride exhibited excellent thermoluminescence dosimetric properties including a simple glow curve structure, good dose linearity, low fading, reproducibility and so on. The material characterization techniques showed that fluorite has a good structural characteristic as required for a luminescent phosphor. The investigated sample shows six individual peaks in the glow curve after deconvolution. LG fluorite is suitable for use in TL dosimetric applications, as evidenced by the high area percentage and good dose linearity of its principal dosimetric peak (DP). The kinetic parameters of the individual peaks are investigated systematically using computerized and experimental methods. The kinetic parameters obtained by the two methods of VHR are in good agreement with each other but are on the higher side when compared to CGCD and approximation methods. The deconvolution results as a function of increased dose direct that the peaks are stable and follow first-order kinetics. The intensity of successive TL falls on an average of 0.4% per cycle of irradiation, readout and annealing. This is an indication that no structural and trapping site variations take place during 10 repeated cycles. A very low fading observed in the complete TL glow curve signal is due to the high stability and the high percentage area of the main dosimetric peak (DP). Pakistani natural calcium fluoride is suitable for practical dosimetry applications including personal and environmental dosimetry. Additional TL and dosimetric applications can be explored if the studied dose range is extended on both lower and higher sides.

5 References:

[1] E. G. Yukihara, S. W. McKeever, C. E. Andersen, A. J. Bos, I. K. Bailiff, E. M. Yoshimura*, et al.*, "Luminescence dosimetry," *Nature Reviews Methods Primers,* vol. 2, pp. 1-21, 2022.

[2] E. G. Yukihara, A. J. Bos, P. Bilski, and S. W. McKeever, "The quest for new thermoluminescence and optically stimulated luminescence materials: Needs, strategies and pitfalls," *Radiation Measurements,* p. 106846, 2022.

[3] C. Sunta, *Unraveling thermoluminescence* vol. 202: Springer, 2014.

[4] R. Chen and S. W. McKeever, *Theory of thermoluminescence and related phenomena : A simulation approach*: World Scientific, 1997.

[5] A. J. J. Bos, "Theory of thermoluminescence," *Radiation Measurements,* vol. 41, pp. S45-S56, 2006.

[6] R. Chen and Y. Kirsh, *The analysis of thermally stimulated processes*: Elsevier, 2013.

[7] S. W. McKeever, *Thermoluminescence of solids* vol. 3: Cambridge University Press, 1988.

[8] S. M. ul Hassan, W. Karam, M. Fakhar-e-Alam, M. Atif, M. Wazir-ud-Din, A. Noureen*, et al.*, "Physical properties of PEG coated Y doped ZnO nanoparticles and their potential as high gamma dose thermoluminescence material," *Journal of King Saud University-Science,* vol. 34, p. 101958, 2022.

[9] S. Hayat, M. T. Siddique, M. Wazir-ud-Din, and M. Jain, "Dosimetric and TL investigation of natural and heat-treated Pakistani Onyx at high beta doses," *Journal of Luminescence,* p. 119178, 2022.

[10] M. A. Atlıhan, "Thermoluminescence properties of two natural colorful fluorite samples of Anatolian origin for dosimetric applications," *Nuclear Instruments and Methods in Physics Research Section B: Beam Interactions with Materials and Atoms,* vol. 467, pp. 33-39, 2020.

[11] Z. Yegingil, N. Nur, T. Dogan, N. Yazici, and M. Topaksu, "Effects of annealing and high radiation dose on the thermoluminescence characteristics of natural fluorite," *Radiation Measurements,* vol. 47, pp. 981-987, 2012.

[12] N. Nur, Z. Yeğingil, M. Topaksu, K. Kurt, T. Doğan, N. Sarıgül*, et al.*, "Study of thermoluminescence response of purple to violet amethyst quartz from Balikesir, Turkey," *Nuclear Instruments and Methods in Physics Research Section B: Beam Interactions with Materials and Atoms,* vol. 358, pp. 6-15, 2015.

[13] M. M. Mahmood, M. B. Kakakhel, M. Wazir-ud-Din, S. Hayat, K. Ahmad, M. T. Siddique*, et al.*, "Thermoluminescence (TL), kinetic parameters and dosimetric features of Pakistani limestone," *Applied Radiation and Isotopes,* vol. 188, p. 110357, 2022.

[14] K. Ahmad, M. B. Kakakhel, S. Hayat, M. Wazir-Ud-Din, M. M. Mahmood, S. Ur-Rehman*, et al.*, "Dosimetric properties of thermoluminescent NaCl pellets from Khewra Salt Mines, Pakistan," *Luminescence,* Jul 21 2022.

[15] M. I. Anjum, S. ur Rehman, M. B. Kakakhel, M. T. Siddique, M. M. Mahmood, S. Hayat*, et al.*, "Thermoluminescence study of Pink Himalayan salt from Khewra mines, Pakistan," *Journal of Luminescence,* p. 119329, 2022.

[16] J. H. Schulman, F. H. Attix, E. J. West, and R. J. Ginther, "New thermoluminescent dosimeter," *Review of Scientific Instruments,* vol. 31, pp. 1263-1269, 1960.

[17] R. Schayes, C. Brooke, I. Kozlowitz, and M. Lheureux, "Thermoluminescent properties of natural calcium fluoride," in *Luminescence Dosimetry, USAEC Conf-650637, US Atomic Energy Commission*, 1967, pp. 138-157.

[18] R. Schayes, M. Lorthioir, and M. Lheureux, "La Dosimetrie par Thermoluminescence," *Revue MBLE,* vol. 6, p. 30, 1963.

[19] C. Brooke and R. Schayes, "Recent Developments in Thermoluminescent Dosimetry; Extensions in the Range of Applications," in *Solid State and Chemical Radiation Dosimetry in Medicine and Biology. Proceedings of a Symposium*, 1967.

[20] C. Sunta, "Thermoluminescence of natural CaF 2 and its applications," 1971.

[21] F. Balogun, J. Ojo, F. Ogundare, M. Fasasi, and L. Hussein, "TL response of a natural fluorite," *Radiation measurements,* vol. 30, pp. 759-763, 1999.

[22] F. Ogundare, F. Balogun, and L. Hussain, "Kinetic characterization of the thermoluminescence of natural fluorite," *Radiation measurements,* vol. 38, pp. 281-286, 2004.

[23] F. Ogundare, F. Balogun, and L. Hussain, "Heating rate effects on the thermoluminescence of fluorite," *Radiation measurements,* vol. 40, pp. 60-64, 2005.

[24] G. Kitis, M. Spiropulu, J. Papadopoulos, and S. Charalambous, "Heating rate effects on the TL glow-peaks of three thermoluminescent phosphors," *Nuclear Instruments and Methods in Physics Research Section B: Beam Interactions with Materials and Atoms,* vol. 73, pp. 367-372, 1993.

[25] T. Calderon, M.-R. Khanlary, H. Rendell, and P. Townsend, "Luminescence from natural fluorite crystals," *International Journal of Radiation Applications and Instrumentation. Part D. Nuclear Tracks and Radiation Measurements,* vol. 20, pp. 475-485, 1992.

[26] M. Topaksu, V. Correcher, and J. Garcia-Guinea, "Luminescence emission of natural fluorite and synthetic CaF2: Mn (TLD-400)," *Radiation Physics and Chemistry,* vol. 119, pp. 151-156, 2016.

[27] T. Calderón, A. Millán, F. Jaque, and J. G. Sole, "Optical properties of Sm2+ and Eu2+ in natural fluorite crystals," *International Journal of Radiation Applications and Instrumentation. Part D. Nuclear Tracks and Radiation Measurements,* vol. 17, pp. 557-561, 1990.

[28] H. Rendell, M.-R. Khanlary, P. Townsend, T. Calderón, and B. Luff, "Thermoluminescence spectra of minerals," *Mineralogical Magazine,* vol. 57, pp. 217-222, 1993.

[29] C. Sunta, "A review of thermoluminescence of calcium fluoride, calcium sulphate and calcium carbonate," *Radiation Protection Dosimetry,* vol. 8, pp. 25-44, 1984.

[30] M. S. Malkani and A. M. K. MH, "New Fluorite and Celestite deposits from Pakistan: Tectonic and Sedimentary Mineral Resources of Indus Basin (Pakistan)-an overview," *Lasbela University Journal of Science & Technology,* vol. 5, pp. 27-33, 2016.

[31] M. S. Malkani and Z. Mahmood, *Fluorite from Loralai-Mekhtar and Celestite from Barkhan, Dera Bugti, Kohlu, Loralai and Musakhel districts (Sulaiman Foldbelt) and Karkh area of Khuzdar district (Kirthar Range): a glimpse on tectonic and sedimentary mineral resources of Indus Basin (Pakistan)*, 2017.

[32] U. Holzwarth and N. Gibson, "The Scherrer equation versus the'Debye-Scherrer equation'," *Nature nanotechnology,* vol. 6, pp. 534-534, 2011.

[33] S. W. McKeever, M. Moscovitch, and P. D. Townsend, "Thermoluminescence dosimetry materials: properties and uses," 1995.

[34] S. Ghias, K. H. Satti, M. Khan, M. Dilband, A. Naseem, A. Jabbar*, et al.*, "Health risk assessment of radioactive footprints of the urban soils in the residents of Dera Ghazi Khan, Pakistan," *Chemosphere,* vol. 267, p. 129171, 2021.

[35] L. Bøtter-Jensen, C. Andersen, G. A. Duller, and A. S. Murray, "Developments in radiation, stimulation and observation facilities in luminescence measurements," *Radiation Measurements,* vol. 37, pp. 535-541, 2003.

[36] T. Lapp, M. Kook, A. S. Murray, K. J. Thomsen, J.-P. Buylaert, and M. Jain, "A new luminescence detection and stimulation head for the Risø TL/OSL reader," *Radiation Measurements,* vol. 81, pp. 178-184, 2015.

[37] M. Sohrabi, F. Abbasisiar, and M. Jafarizadeh, "Dosimetric Characteristics of Natural Calcium Fluoride of Iran," *Radiation Protection Dosimetry,* vol. 84, pp. 277-280, 1999.

[38] M. Topaksu and A. N. Yazici, "The thermoluminescence properties of natural CaF2 after β-irradiation," *Nuclear Instruments and Methods in Physics Research Section B: Beam Interactions with Materials and Atoms,* vol. 264, pp. 293-301, 2007.

[39] C. Sunta, "Thermoluminescence spectrum of gamma-irradiated natural calcium fluoride," *Journal of Physics C: Solid State Physics,* vol. 3, p. 1978, 1970.

[40] M. Chougaonkar and B. Bhatt, "Blue light stimulated luminescence in calcium fluoride, its characteristics and implications in radiation dosimetry," *Radiation protection dosimetry,* vol. 112, pp. 311-321, 2004.

[41] E. Mische and S. McKeever, "Mechanisms of supralinearity in lithium fluoride thermoluminescence dosemeters," *Radiation protection dosimetry,* vol. 29, pp. 159-175, 1989.

[42] C. Furetta, M. Prokic, R. Salamon, and G. Kitis, "Dosimetric characterisation of a new production of MgB4O7: Dy, Na thermoluminescent material," *Applied Radiation and Isotopes,* vol. 52, pp. 243-250, 2000.

[43] J. A. Harvey, K. J. Kearfott, and M. Rafique, "Dose response linearity and practical factors influencing minimum detectable dose for various thermoluminescent detector types," *Journal of Radioanalytical and Nuclear Chemistry,* vol. 303, pp. 1711-1718, 2015.

[44] C. Furetta, *Handbook of thermoluminescence*: World Scientific, 2010.

[45] L. S. Meireles, M. A. S. Lacerda, L. C. Meira-Belo, and H. R. Ferreira, "Study of the influence of the time temperature profile on the minimum detectable dose of TLD-100," 2013.

[46] M. Latif, M. Fasasi, and F. Balogun, "Low dose TL characteristics of Nigerian fluorite," *Radiation measurements,* vol. 47, pp. 182-184, 2012.

[47] S. W. McKeever, "On the analysis of complex thermoluminescence. Glow-curves: Resolution into individual peaks," *physica status solidi (a),* vol. 62, pp. 331-340, 1980.

[48] K. H. Gavhane, M. S. Bhadane, A. S. Bhoir, P. P. Kulkarni, B. J. Patil, V. N. Bhoraskar*, et al.*, "Tm-Tstop analysis and dosimetric properties of Ce doped BaB4O7 phosphor," *Journal of Alloys and Compounds,* vol. 817, p. 152805, 2020.

[49] P. P. Kulkarni, K. H. Gavhane, M. S. Bhadane, V. N. Bhoraskar, S. S. Dahiwale, and S. D. Dhole, "Investigation of thermoluminescence and photoluminescence properties of Tb 3+, Eu 3+, and Dy 3+ doped NaYF 4 phosphors for dosimetric applications," *Physical Chemistry Chemical Physics,* vol. 24, pp. 11137-11150, 2022.

[50] K. H. Gavhane, M. S. Bhadane, P. P. Kulkarni, V. Bhoraskar, S. Dhole, and S. Dahiwale, "Investigation of novel Eu doped SrDy2O4 microphosphor for thermoluminescence dosimetry," *Journal of Luminescence,* vol. 231, p. 117781, 2021.

[51] P. P. Kulkarni, K. H. Gavhane, M. S. Bhadane, V. N. Bhoraskar, S. S. Dahiwale, and S. D. Dhole, "Investigation of the photoluminescence and novel thermoluminescence dosimetric properties of NaGdF 4: Tb 3+ phosphors," *Materials Advances,* vol. 1, pp. 1113-1124, 2020.

[52] Y. Horowitz and M. Moscovitch, "Highlights and pitfalls of 20 years of application of computerised glow curve analysis to thermoluminescence research and dosimetry," *Radiation protection dosimetry,* vol. 153, pp. 1-22, 2013.

[53] Y. S. Horowitz and D. Yossian, *Computerised glow curve deconvolution: application to thermoluminescence dosimetry*: Nuclear Technology Publ., 1995.

[54] M. Wazir-ud-Din, S. ur-Rehman, M. M. Mahmood, K. Ahmad, S. Hayat, M. T. Siddique*, et al.*, "Computerized glow curve deconvolution (CGCD): A comparison using asymptotic vs rational approximation in thermoluminescence kinetic models," *Applied Radiation and Isotopes,* vol. 179, p. 110014, 2022/01/01/ 2022.

[55] R. Chen and S. W. McKeever, *Theory of thermoluminescence and related phenomena*: World Scientific, 1997.

[56] H. G. Balian and N. W. Eddy, "Figure-of-merit (FOM), an improved criterion over the normalized chi-squared test for assessing goodness-of-fit of gamma-ray spectral peaks," *Nuclear Instruments and Methods,* vol. 145, pp. 389-395, 1977.

[57] W. Hoogenstraaten, "Electron traps in zinc sulphide phosphors," *Philips Research Report,* vol. 13, pp. 515-693, 1958.